VV 655 and NGC 4418: Implications of an interaction for the evolution of a LIRG

A&A 637, A17 (2020)
https://doi.org/10.1051/0004-6361/201834880

Astronomy & Astrophysics

VV 655 and NGC 4418: Implications of an interaction for the evolution of a LIRG⋆

Erin Boettcher[1,2], John S. Gallagher III[1], Youichi Ohyama[3], Eskil Varenius[4], Susanne Aalto[5], Niklas Falstad[5], Sabine König[5], Kazushi Sakamoto[3], and Tova M. Yoast-Hull[6]

[1] Department of Astronomy, University of Wisconsin-Madison, 475 N. Charter St., Madison, WI 53706, USA
e-mail: jsg@astro.wisc.edu
[2] Department of Astronomy and Astrophysics, University of Chicago, 5640 S. Ellis Ave., Chicago, IL 60637, USA
e-mail: eboettcher@astro.uchicago.edu
[3] Institute of Astronomy and Astrophysics, Academia Sinica, 11F of Astronomy-Mathematics Building, AS/NTU, No. 1, Sec. 4, Roosevelt Rd., Taipei 10617, Taiwan, ROC
[4] Jodrell Bank Centre for Astrophysics, School of Physics and Astronomy, The University of Manchester, Alan Turing Building, Oxford Road, Manchester M13 9PL, UK
[5] Department of Space, Earth and Environment, Onsala Space Observatory, Chalmers University of Technology, 439 92 Onsala, Sweden
[6] Canadian Institute for Theoretical Astrophysics, University of Toronto, 60 St. George St., Toronto, ON M5S 3H8, Canada

Received 14 December 2018 / Accepted 5 March 2020

ABSTRACT

Context. VV 655, a dwarf irregular galaxy with HI tidal debris, is a companion to the lenticular luminous infrared galaxy (LIRG) NGC 4418. NGC 4418 stands out among nearby LIRGs due to its dense central concentration of molecular gas and the dusty, bi-polar structures along its minor axis suggestive of a wind driven by a central starburst and possible nuclear activity.
Aims. We seek to understand the consequences of the ongoing minor interaction between VV 655 and NGC 4418 for the evolution of the LIRG. Specifically, we consider the origin of the gas supply responsible for the unusual nuclear properties of NGC 4418.
Methods. We investigate the structural, kinematic, and chemical properties of VV 655 and NGC 4418 by analyzing archival imaging data and optical spectroscopic observations from the SDSS-III and new spectra from SALT-RSS. We characterize their gas-phase metal abundances and spatially resolved, ionized gas kinematics to better understand whether gas transfer between VV 655 and NGC 4418 resulted in the highly obscured nucleus of the LIRG.
Results. The gas-phase metallicity in NGC 4418 significantly exceeds that in VV 655. No kinematic disturbances in the ionized gas are observed along the minor axis of NGC 4418, but we see evidence for ionized gas outflows from VV 655 that may increase the cross-section for gas stripping in grazing collisions. A faint, asymmetric outer arm is detected in NGC 4418 of the type normally associated with galaxy-galaxy interactions.
Conclusions. The simplest model suggests that the minor interaction between VV 655 and NGC 4418 produced the unusual nuclear properties of the LIRG via tidal torquing of the interstellar medium of NGC 4418 rather than through a significant gas transfer event. In addition to inducing a central concentration of gas in NGC 4418, this interaction also produced an enhanced star formation rate and an outer tidal arm in the LIRG. The VV 655-NGC 4418 system offers an example of the potential for minor collisions to alter the evolutionary pathways of giant galaxies.

Key words. galaxies: individual: NGC 4418 – galaxies: individual: VV 655 – galaxies: ISM – ISM: kinematics and dynamics – ISM: jets and outflows – galaxies: interactions

1. Introduction

VV 655 is a gas-rich dwarf irregular galaxy that is interacting with NGC 4418, its lenticular luminous infrared galaxy (LIRG) companion (Armus et al. 1987; Varenius et al. 2017). While galaxy-galaxy interactions, such as major mergers, are widely studied as important evolutionary factors, the diversity of interactions between gas-rich dwarf and giant galaxies is yet to be systematically explored. Even so, it is clear that minor mergers ($\lesssim$1:10 mass ratio) can fuel central activity in giant galaxies (e.g., see Duprie & Schneider 1996; Pisano & Wilcots 1999; Aalto et al. 2001; Balcells et al. 2001; Ferreiro & Pastoriza 2004; Koribalski & Manthey 2005; Sancisi et al. 2008; Knierman 2010; Pearson et al. 2018). While simulations and observations underscore the importance of minor mergers as drivers of galaxy evolution, the impact of minor interactions that do not involve mergers is less well studied, especially from an observational perspective. These types of processes are difficult to detect, especially in galaxies at cosmological distances, and can help to explain the presence of LIRGs with apparently undisturbed structures that are seen out to at least moderate redshifts (e.g., Pereira-Santaella et al. 2019).

NGC 4418 has several unusual nuclear properties, including a deep mid-infrared silicate absorption feature produced by cold dust (Roche et al. 1986, 2015; Spoon et al. 2001) and an extraordinarily dense ($n(H_2) = 10^5 - 10^7$ cm^{-3}; Costagliola et al. 2015) central concentration of $\sim 10^8\,M_\odot$ of molecular gas (Kawara et al. 1990; Aalto et al. 2007; Lahuis et al. 2007; Imanishi et al. 2010; Sakamoto et al. 2010;

⋆ Based in part on observations made with the Southern African Large Telescope (SALT) as part of program 2014-2-SCI-052 (P.I.: J. S. Gallagher).

Table 1. Properties of VV 655 and NGC 4418.

	VV 655		NGC 4418		
Observed property	Measured	Physical	Measured	Physical	Notes
RA (J2000)	$12^h27^m04\overset{s}{.}56$		$12^h26^m54\overset{s}{.}62$		(*a*)
Dec (J2000)	$-00^d54^m23\overset{s}{.}2$		$-00^d52^m39\overset{s}{.}4$		(*a*)
Redshift	2202 km s^{-1}	34 Mpc	2106 km s^{-1}	34 Mpc	(*b*)
Far-UV Mag.	16.8	4×10^{42} erg s^{-1}	...	...	(*c*)
3.6 μm Mag.	12.5	$2.4\times10^9\,L_\odot$	9.9	$2.7\times10^{10}\,L_\odot$	(*d*)
HI Mass	$1\times10^9\,M_\odot$	M(HI)/$M_*\approx1/2$	...	...	(*e*)
$R_P(r)$	18″	3.0 kpc	27″	4.3 kpc	(*f*)
v_{rot}	20 km s^{-1}	30–90 km s^{-1}	130 km s^{-1}	150 km s^{-1}	(*g*)
SFR		~0.1 $M_\odot$ yr^{-1}		~3.2 $M_\odot$ yr^{-1}	(*h*)

Notes. [(a)]From the NASA/IPAC Extragalactic Database (NED; https://ned.ipac.caltech.edu/). [(b)]Systemic HI velocity from Varenius et al. (2017). [(c)]From GALEX archival images, this paper; NGC 4418 is on the edge of the GALEX field of view and thus its FUV magnitude is not given. [(d)]From *Spitzer* archival images, this paper. [(e)]HI mass from Varenius et al. (2017), measured over the region shown in their Fig. 5; the HI content of NGC 4418 is not well determined due to HI absorption. Stellar mass from $L_{3.6}$ assuming M/L = 1. [(f)]r-band Petrosian radius from SDSS-III DR 12. [(g)]From Varenius et al. (2017) and this paper (VV 655) and Ohyama et al. (2019; NGC 4418). [(h)]From Varenius et al. (2017), as derived from the 1.4 GHz continuum, and this paper.

González-Alfonso et al. 2012; Costagliola et al. 2015), including an extremely Compton-thick nuclear region (N(H) $\gtrsim 10^{25}$ cm^{-2}; Sakamoto et al. 2013). Kpc-scale bipolar dust filaments extend from the central regions of NGC 4418 (Evans et al. 2003; Sakamoto et al. 2013; Ohyama et al. 2019), which contain a post-starburst stellar population as well as a possible highly obscured AGN (Roche et al. 1986; Evans et al. 2003; Shi & Gu 2005; Sakamoto et al. 2013; Ohyama et al. 2019, see also Sect. 4). These features suggest that an influx of interstellar matter reached the central zones of NGC 4418 within the past ~Gyr, leading to enhanced star formation for at least the last 300 Myr (Shi & Gu 2005; Ohyama et al. 2019) and possibly fueling AGN activity.

The general properties of NGC 4418, including a centrally concentrated power source, substantial molecular medium, and clear presence of dust, are found in a significant fraction (~1/10–1/4) of early-type field galaxies (e.g., Koda et al. 2005; Kaviraj et al. 2012; Nyland et al. 2017). However, NGC 4418 stands out in terms of its status as a LIRG, the extreme density of its circum-nuclear molecular medium, and its ongoing interaction with VV 655, evidenced by the HI bridge connecting the galaxies (Varenius et al. 2017; see Table 1 for a summary of the properties of these galaxies). This presents the possibility that either a gas transfer event or tidal torquing of the interstellar medium (ISM) of the LIRG has shaped the nuclear properties of NGC 4418. A variety of studies, including those focusing on early-type galaxies with molecular interstellar matter by Lucero & Young (2013) and O'Sullivan et al. (2018), emphasize the importance of minor mergers and interactions in producing present-day examples of gas-rich, early-type galaxies. NGC 4418 and VV 655 thus present a crucial case study for better understanding the mechanisms by which minor interactions can shape the evolutionary trajectories of gas-rich dwarf and giant galaxy pairs.

In this brief communication, we explore the connection between the minor interaction of NGC 4418 with VV 655 and the nuclear properties of the LIRG based on a combination of archival, multi-wavelength observations and a longslit spectrum obtained with the Southern African Large Telescope (SALT). The next section presents the observations, which we analyze in Sect. 3. In particular, we address whether there is evidence for low-metallicity gas from VV 655 residing within NGC 4418. We also examine the ionized gas kinematics to search for evidence of gas accretion onto NGC 4418 and ionized gas outflows from VV 655 that could be feeding gas onto its companion. In Sect. 4, we explore possible connections between the interaction with VV 655 and the unusual properties of NGC 4418, including a comparison of the relevant timescales. Section 5 contains a discussion of the results and our conclusions. We adopt a distance of 34 Mpc for the VV 655–NGC 4418 system, giving a scale of 160 pc arcsec^{-1}.

2. Observations

2.1. Spectroscopy

We conducted our analysis using complementary spectroscopic data sets from the Sloan Digital Sky Survey III (SDSS-III; Sect. 2.1.1) and SALT (Sect. 2.1.2). As detailed below, the SDSS-III single-fiber spectra provide broad wavelength coverage ($\lambda \sim$ 3800–9200 Å) and excellent flux calibration in the central regions of the galaxies only. In contrast, the SALT longslit observations offer spatially resolved spectroscopy across both galaxies over a more limited wavelength range ($\lambda \sim$ 5560–6840 Å) at somewhat improved spectral resolution ($R \sim$ 2500 vs. 2000 near Hα).

2.1.1. Data from the Sloan Digital Sky Survey III

The SDSS-III data release 12 (DR 12) Science Archive Server includes reduced spectra of VV 655 (Object ID: 12376487 20159965325, Plate: 0289, MJD: 51990, Fiber: 0202) and NGC 4418 (Object ID: 1237648720159965190, Plate: 0289, MJD: 51990, Fiber: 0208)[1]. These spectra were taken with 3″ diameter fibers whose locations are shown in Fig. 1. In Table 2, we reproduce the emission-line ratios determined from the SDSS-III Portsmouth spectroscopic re-analysis for both galaxies. The reduced spectra extend redwards from approximately 3800 Å and therefore miss the [OII]λ3727 doublet.

[1] http://skyserver.sdss.org/dr12/en/tools/explore/summary.aspx

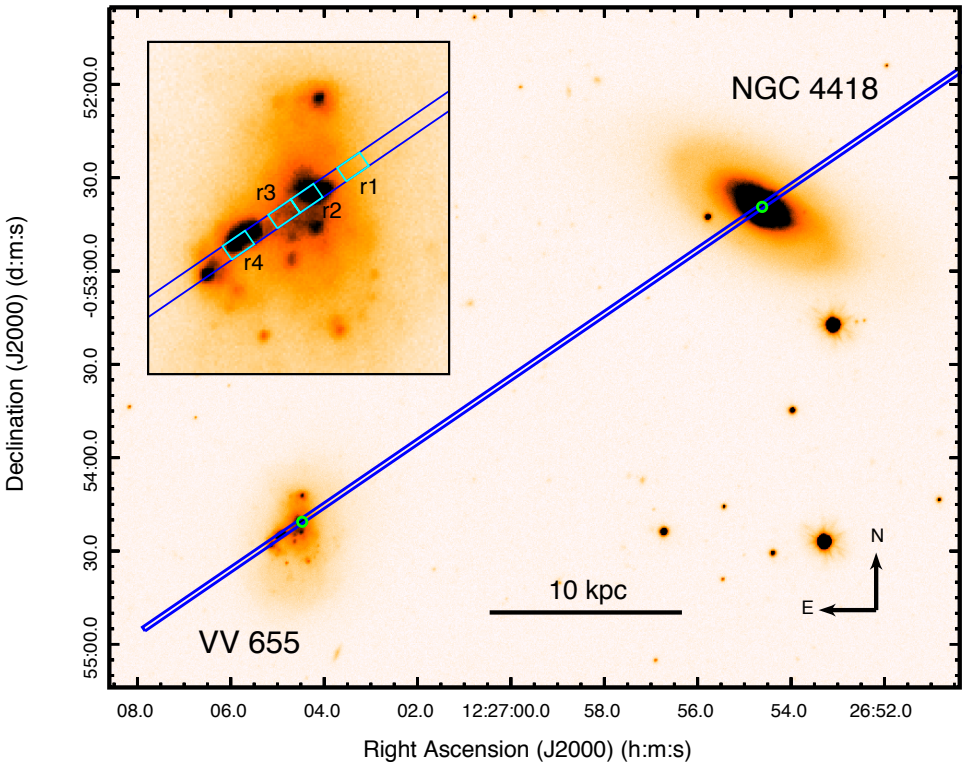

Fig. 1. VV 655 and NGC 4418 illustrated in a reproduction of a KiDS DR4 g-band archival image (Kuijken et al. 2019); the galaxies are separated by a projected distance of 184″ (30 kpc). The SALT-RSS longslit is shown in blue, and the SDSS fibers are indicated in green. The inset shows the locations of r1–r4 on an enlarged image of VV 655. The SALT observations allow the gas-phase chemical abundances and any kinematic disturbances in the ionized gas to be characterized across the bodies of both galaxies.

Table 2. Emission-line ratios for VV 655 and NGC 4418.

Galaxy	[OIII]λ5007/Hα	[NII]λ6583/Hα	[SII]λ6716/Hα	[SII]λ6716/[SII]λ6731	Notes
			SDSS-III		
VV 655	0.62 ± 0.01	0.098 ± 0.004	0.150 ± 0.005	1.43 ± 0.07	(*a*)
NGC 4418	0.17 ± 0.04	0.95 ± 0.05	0.47 ± 0.04	1.2 ± 0.1	(*a*)
			SALT-RSS		
VV 655 (r1; Diffuse)	...	0.121 ± 0.007	0.230 ± 0.007	1.52 ± 0.08	
VV 655 (r2: SF)	...	0.100 ± 0.002	0.170 ± 0.003	1.43 ± 0.04	
VV 655 (r3; Diffuse)	...	0.105 ± 0.003	0.163 ± 0.003	1.35 ± 0.04	
VV 655 (r4: SF)	...	0.091 ± 0.001	0.158 ± 0.001	1.43 ± 0.02	
NGC 4418 (Nucleus)	...	1.27 ± 0.08	0.42 ± 0.06	1.1 ± 0.2	(*b*)
NGC 4418 (R = 7.5″)	...	0.7 ± 0.1	0.45 ± 0.09	1.0 ± 0.3	(*b*)

Notes. [(a)]Emission-line intensities and uncertainties are from the Portsmouth spectroscopic re-analysis presented on the SDSS-III DR 12 Science Archive Server (`http://skyserver.sdss.org/dr12/en/tools/explore/summary.aspx`). [(b)]The continuum in the Hα region of NGC 4418 is corrected for a broad stellar absorption line of strength ~2.5 Å (see Fig. 4).

For VV 655, the ratio of I(Hα)/I(Hβ) = 3.6 observed by SDSS is an upper limit since Hβ emission is more strongly affected by underlying stellar absorption than Hα emission. As a fiducial, we adopt an equivalent width for stellar absorption of 3 Å for the stellar Hα and Hβ lines (Gallagher & Hunter 1987). Assuming that these add directly to the observed line intensities gives I(Hα)/I(Hβ) = 3.0, consistent with the values from model fits in the SDSS `emissionLinesPort` tabulation. This leads to an estimate of $E(B-V) \lessapprox 0.1$ mag for the internal reddening (e.g., Garn & Best 2010), where the foreground reddening is $E(B-V) = 0.07$ mag. We do not perform a reddening correction to the emission-line ratios discussed here due to the small size of this correction and its uncertainty in a likely complex, clumpy medium.

2.1.2. Spectra from the Southern African Large Telescope

A longslit spectrum of VV 655 and NGC 4418 was taken on March 15, 2015 with the Robert Stobie Spectrograph (RSS) on SALT as part of program 2014-2-SCI-052 (P.I.: J. S. Gallagher). The 2 × 1250 s observations used a 1.5″ slit width in combination with the PG1800 VPH grating. We selected a slit position angle of 304.5° such that VV 655 was covered near the south-eastern end of the 8′ longslit as shown in Fig. 1. The slit extends approximately along the minor axis of NGC 4418 and across VV 655, thereby offering a direct, spatially resolved comparison of their emission-line intensities and gas kinematics. In VV 655, the SALT spectrum samples a 6 kpc swath across the galaxy, in contrast to the 0.5 kpc sampled by the SDSS fiber that contains ≲10% of the total light.

We used the PySALT science pipeline[2] to perform a series of corrections (bias, gain, and cross-talk) and to prepare and mosaic the six frames that constitute each spectrum (Crawford et al. 2010). We then removed cosmic rays using the `L.A.Cosmic` task in IRAF[3] (van Dokkum 2001). Using Ar comparison lamp spectra, we determined the dispersion solution using the `noao.twodspec.longslit.identify`, `.reidentify`, `.fitcoords`, and `.transform` tasks.

We used the IRAF task `images.immatch.imcombine` to perform a median image stack with median scaling and weighting. To remove the sky lines, we extracted and subtracted sky-line spectra from portions of the slit free from object contamination. We calculated the uncertainty per pixel by propagating the Poisson error through the reduction process.

We extracted spectra along the regions of interest around VV 655 and NGC 4418 using a median combination over an 11 pixel (~450 pc) aperture. We calculated the emission-line intensities by integrating over the lines of interest in the continuum-subtracted spectra. The NGC 4418 spectra show evidence of a broad stellar absorption feature at Hα, which we fit and removed with an absorption line of equivalent width ~2.5 Å. The uncertainties on the measured intensities account for the Poisson error and a 5% error on the continuum.

To characterize their kinematics, we fit the emission lines of interest with single Gaussians using the IDL `gaussfit` function. This function uses a least-squares approach to determine the best-fit line centers, widths, and amplitudes and the uncertainties on these parameters. In instances where two Gaussian components are required to sufficiently represent the emission-line profile, we performed the multi-component fit by minimizing the chi-squared statistic ($\chi^2 = \Sigma_{i=0}^{N} \frac{(I_{\lambda,\mathrm{obs},i} - I_{\lambda,\mathrm{mod},i})^2}{\sigma^2_{\lambda,\mathrm{obs},i}}$) over a grid in parameter space, where $I_{\lambda,\mathrm{obs},i}$ and $I_{\lambda,\mathrm{mod},i}$ are the observed and modeled flux densities of the ith pixel and $\sigma_{\lambda,\mathrm{obs},i}$ is the uncertainty on the former quantity.

We thus characterized the emission-line intensities in instrumental units, radial velocities, and velocity dispersions as functions of position along the slit within both galaxies. All radial velocities presented in this paper are heliocentric velocities determined using the IRAF task `astutil.rvcorrect`. All line widths are corrected for the instrumental resolution determined from the comparison lamp spectra.

2.2. Imaging and photometry

Archival images and photometry of VV 655 and NGC 4418 are available from several sources; some of the derived properties of these galaxies are summarized in Table 1. As shown in Fig. 2, the ultraviolet (UV) structure of VV 655 shows multiple UV-bright starforming regions, consistent with the spatially extended emission lines observed in our SALT spectrum (see Sect. 3). Thus, while the outer isophotes of VV 655 are fairly regular, the star formation in this galaxy is found in multiple, discrete clumps, suggestive of the irregular elliptical (iE) class of blue compact dwarf galaxies (e.g., Loose & Thuan 1986).

For VV 655, we measured integrated magnitudes from GALEX far-UV (FUV) and *Spitzer* 3.6 μm band-1 images (see Fig. 2). The *Spitzer* 3.6 μm luminosity is $\sim 3 \times 10^9\, L_\odot$, which yields a stellar mass estimate of a few $\times 10^9\, M_\odot$. For comparison, the gas mass associated with VV 655 is $\sim 1 \times 10^9\, M_\odot$ (Varenius et al. 2017), and thus despite the loss of a considerable gas mass, VV 655 remains quite gas-rich.

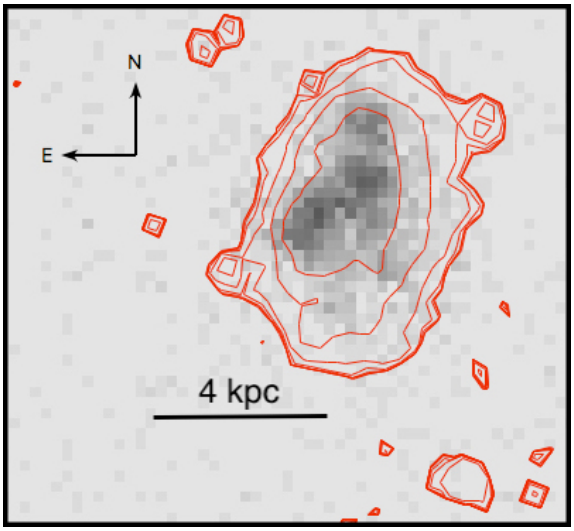

Fig. 2. Structure of the stellar body of VV 655 shown by the GALEX far-UV image (grayscale) with overplotted contours from a *Spitzer* Space Telescope 3.6 μm band-1 image. The outer isophote of VV 655 corresponds to $\approx$22.7 mag arcsec^{-2} ($\approx 10\, L_\odot$ pc^{-2}) and is relatively symmetric with no indication of tidal tails (see also Fig. 1).

The star formation rate of VV 655 derived from the FUV luminosity using the calibration of Kennicutt & Evans (2012) is ~0.1 $M_\odot$ yr^{-1}, assuming $E(B-V) = 0.07$. This result is in good agreement with the star formation rate reported by Varenius et al. (2017). Despite its prominent young stellar population and substantial gas loss during the interaction with NGC 4418, VV 655 retains a sufficient gas supply to support star formation for approximately an additional Hubble time and thus displays star formation properties that are typical of dwarf irregular systems (Hunter & Gallagher 1985; van Zee 2001).

Since it is known that VV 655 and NGC 4418 are interacting (e.g., Varenius et al. 2017), we investigated whether the stellar bodies of either galaxy show evidence for associated tidal distortions. The young stellar population of VV 655 as observed in the FUV is centrally concentrated, while the outer isophotes in the infrared are relatively symmetric with no clear indication of tidal tails. Deeper observations, however, are required to determine the degree to which the tidal debris from VV 655 lacks stars.

Figure 3 shows the g-band KiDS image of NGC 4418 (Kuijken et al. 2019) with a model of the galaxy disk subtracted to display an arm-like feature on the southwest side of the galaxy. To construct the disk profile, we made a smooth model of the light distribution using the IRAF task `ellipse`. The bright star that is projected against the galaxy to the east was effectively removed by adopting the median option for deriving the isophote levels. We used the bmodel capability in `ellipse` to produce a symmetric model of the light distribution that we subtracted from the original image to show the substructure. As the arm-like feature is diffuse, we smoothed the original image with a $\sigma = 3$ pixels (1.2″) Gaussian kernel to improve the signal-to-noise ratio before subtracting the model.

The arm-like structure revealed by this analysis is faint; its contrast with respect to the surrounding disk is 5–10% and it is detected at the 5–10σ level relative to the background after model subtraction. The visible part of this feature, which we will

[2] http://pysalt.salt.ac.za/

[3] IRAF is distributed by the National Optical Astronomy Observatories, which are operated by the Association of Universities for Research in Astronomy, Inc., under cooperative agreement with the National Science Foundation.

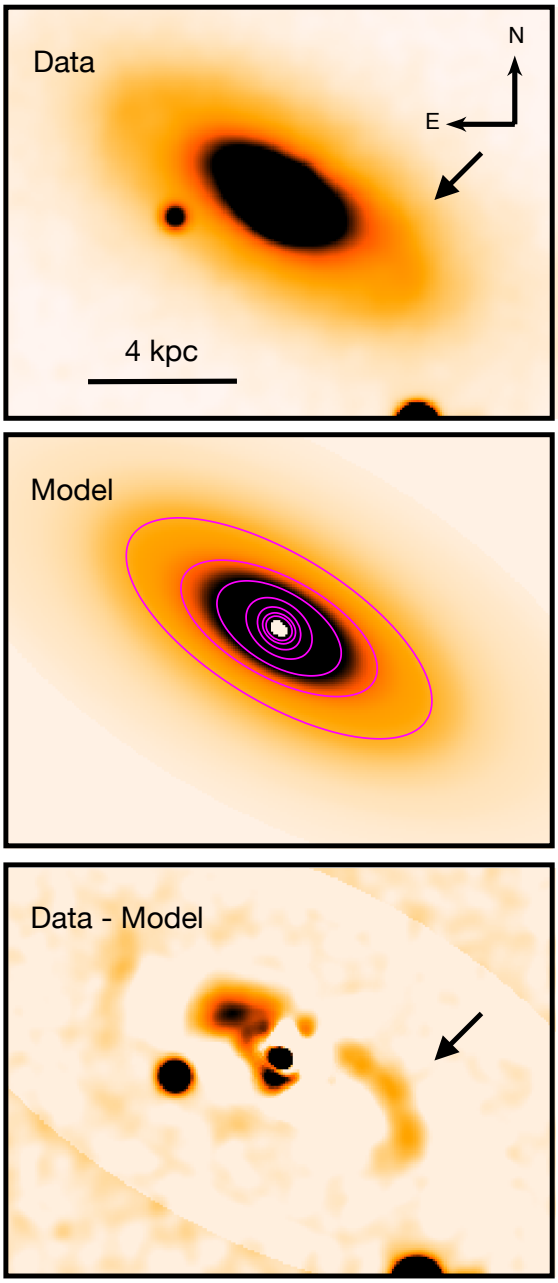

Fig. 3. g-band image of NGC 4418 from the KiDS archive (Kuijken et al. 2019) illustrating the internal structure of the outer disk before (*top*) and after (*bottom*) subtraction of a disk model (*middle*). The images are smoothed with a $\sigma = 3$ pixels (1.2″) Gaussian kernel to improve the signal-to-noise ratio. The difference image reveals an asymmetric feature, indicated by the arrow, that has the properties of a one-sided tidal tail produced by a minor interaction. From the inside out, the contour levels in the *middle panel* are at 80%, 60%, 40%, 20%, 10%, and 5% of the surface brightness of the innermost contour. The central pixels in NGC 4418 are excluded from the model fit due to dust structures at this location. The features near the center of the galaxy in the bottom panel are due to undersubtraction of the smooth model from the centrally complex, clumpy data.

refer to as the "outer arm" (see below), contains ∼1% of the total R-band flux from the galaxy. At a projected distance of ∼4 kpc from the center, the width of the outer arm is ≈6″, or ≈1 kpc. It is asymmetric in that a counterpart is not detected on the opposite side of the galaxy. Since the stellar rotation of the southwest side of NGC 4418 is redshifted (see Fig. 6 of Ohyama et al. 2019) and extinction by a dusty polar outflow along the northwest semi-minor axis suggests that the northwest side of the galactic disk is the far side (Sakamoto et al. 2013; Ohyama et al. 2019), the arm-like feature appears to be a trailing structure, as expected. For this reason, we favor the interpretation of this feature as a disk structure rather than a projected tidal stream in the halo.

The outer arm is also visible in the SDSS-III images, but its presence to our knowledge has not been noted in the literature. However, NGC 4418 has sometimes been classified as an Sa galaxy with an outer ring. The presence of an outer ring is not confirmed in modern data, but it is possible that the arm-like feature in NGC 4418 was detected but incorrectly interpreted in some of the earlier studies[4].

3. Ionized gas

3.1. Chemical abundances

We quantify and compare the gas-phase metallicities in VV 655 and NGC 4418 to explore the implications for gas transfer events(s) between these galaxies. Our measured oxygen abundance for the ionized gas in VV 655 is based on the strong emission-line abundance calibration developed from SDSS spectra by Curti et al. (2017, see their Fig. 9). Using emission-line intensities for VV 655 from the SDSS single-fiber spectrum, we find the index $\log(N_2) = -1.01 \pm 0.02$, corresponding to $[O/H] = -0.3 \pm 0.1$ or about 40−60% of the solar value (Asplund et al. 2009)[5]. The abundance based on the ratio of I([OIII]λ5007) to I(Hβ) gives a similar result with an abundance of ∼60% of solar in the MPA-JHU galaxy properties catalog[6].

Using the SALT spectra, we quantify the spatially resolved emission-line ratios in four regions of VV 655 – two star-forming (r2 and r4) and two diffuse regions (r1 and r3; see Fig. 1). As reported in Table 2, the [SII] doublet intensity ratio is close to the low-density limit, indicating that most of the observed emission is coming from HII regions and surrounding diffuse ionized gas. The low characteristic value of $\log(N_2) = -1.0 \pm 0.01$ and [NII] intensities below those of [SII] agree with a metallicity approaching that of the Small Magellanic Cloud (SMC) across the body of VV 655. Thus, both the SDSS-III and SALT observations indicate that the gas-phase metallicity in VV 655 is distinctly sub-solar, suggesting that this galaxy is not a remnant of what was once a considerably more massive galaxy and is unlikely to have been heavily disrupted by its interaction with NGC 4418.

As shown in Fig. 4 and Table 2, the emission-line ratios of the ionized gas in VV 655 markedly differ from those of the extended ionized medium in its LIRG companion. For NGC 4418, we report SALT measurements at the location of the optical continuum intensity peak (labeled nucleus) and at the largest distance from the center at which a spectrum with sufficient signal-to-noise ratio could be extracted ($R = 7.5''$ or 1.2 kpc to the northwest). It is clear that the characteristic value of $\log(N_2) = 0.0 \pm 0.04$ observed in NGC 4418 is a dex larger than that seen in VV 655; this value is consistent with that found from the SDSS spectrum within the uncertainties. The ionized gas along the south-southeast minor axis of NGC 4418 in

[4] The Uppsala General Catalog of Galaxies (Nilson 1973) classifies NGC 4418 as an Sa galaxy and notes the presence of a superimposed companion that we suspect is the tidal arm feature.
[5] N_2 is the intensity ratio between the [NII]λ6583 and Hα emission lines.
[6] https://www.sdss.org/dr12/spectro/galaxy_mpajhu/

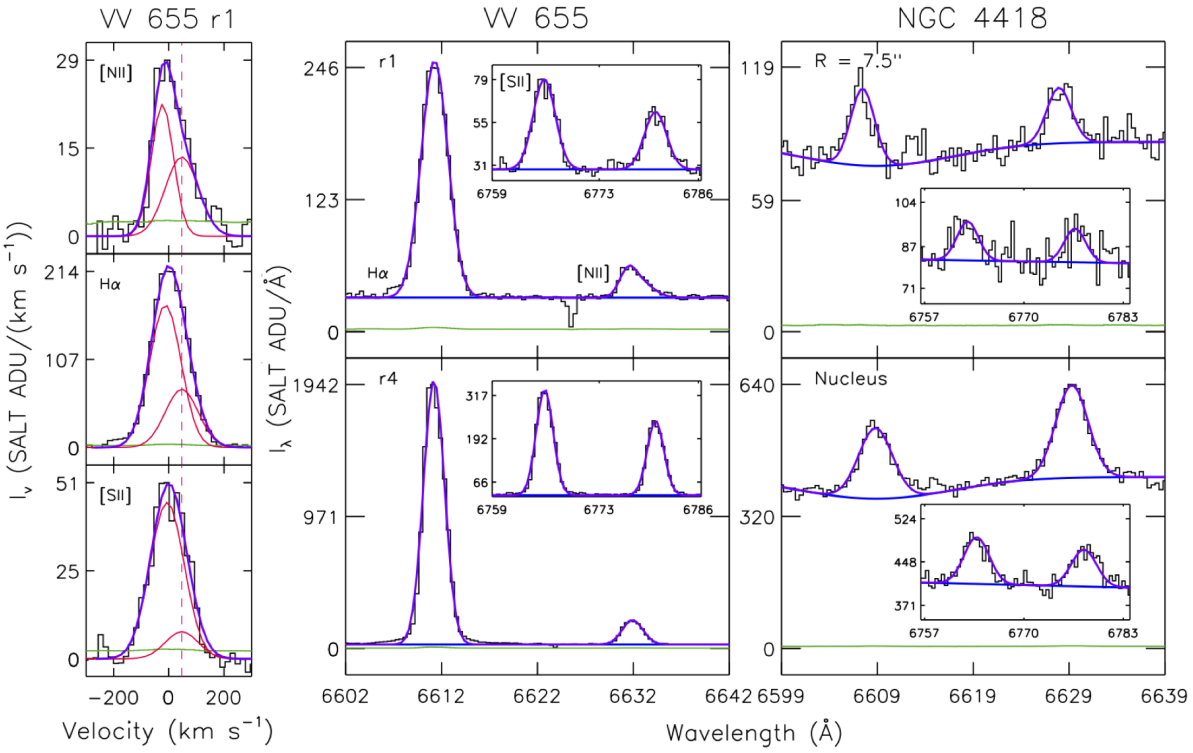

Fig. 4. SALT-RSS spectra of emission lines in the Hα region from VV 655 (*left*) and NGC 4418 (*right*). The blue and purple lines indicate fits to the continuum and the single- and multi-component Gaussian emission-line profiles, respectively. The green curves indicate the error spectra. Spectra are shown for a diffuse (r1) and a star-forming region (r4) in VV 655 and near the nucleus and at an offset of $R = 7.5''$ (1.2 kpc) to the northwest in NGC 4418. The difference in the N_2 value of approximately an order of magnitude between the galaxies suggests that the metallicity of the outflowing, ionized gas in NGC 4418 exceeds that of the HII regions in VV 655. As shown at left, in the diffuse regions of VV 655, a redshifted [NII]λ6583 wing extends beyond the velocity range where there are currently HI detections (Varenius et al. 2017). We indicate upper limits on the corresponding kinematic components in the Hα and [SII]λ6716 emission lines, which suggest that the redshifted component arises from gas with an N_2 intensity ratio that exceeds the characteristic value for VV 655 by at least a factor of two. Thus, this feature likely indicates the presence of a shocked, ionized gas outflow. The wavelengths shown are the observed wavelengths. The feature near $\lambda = 6624$ Å is an instrumental artifact.

the direction towards VV 655 has emission-line ratios consistent with ionized gas elsewhere in the galaxy. Ohyama et al. (2019) also find $N_2 \gtrsim 1$ in the extended ionized medium of the galactic outflow, and their independent analysis of the red emission lines in NGC 4418 agrees with our conclusion that the chemical abundance of the ionized gas is near solar values.

Since the material of greatest interest – that of the ionized outflow from the nucleus of NGC 4418 – may be excited by shocks, chemical abundances based on emission-line observations must be considered with care. The optical spectra of supernova remnants in the SMC, where shock excitation is an important factor, have high N_2 values above those of HII regions but less than unity, and a similar result is also found in the Large Magellanic Cloud (Payne et al. 2007, 2008). As the shock-excited supernova remnants in the Magellanic Clouds bracket the likely chemical abundances in VV 655 and have $N_2 < 1$, we conclude that the ionized gas in NGC 4418 has higher metallicity than the HII regions in VV 655.

3.2. Ionized gas kinematics in NGC 4418

The velocity pattern traced by the red [NII] line in the NGC 4418 SALT spectrum is consistent with that found by Ohyama et al. (2019), with radial velocity slowly increasing along the minor axis from the northwest to the southeast. Although our SALT spectroscopy extends across the HI bridge connecting VV 655 and NGC 4418, we do not detect emission to appreciably larger distances toward VV 655 than Ohyama et al. (2019) (~10–15″ or 1.6–2.4 kpc toward the dwarf galaxy; see their Fig. 4). Neither work suggests strong evidence for a direct disturbance of the ionized gas envelope in NGC 4418 associated with the HI tidal debris from VV 655. We do not detect emission lines at the location of the HI bridge between the two galaxies. As the tidal material is extended along an orbit that likely has at most moderate eccentricity, any gas donated from VV 655 must interact and lose angular momentum to reach the center of NGC 4418.

3.3. Galactic outflow from VV 655?

Figure 4 shows a redshifted velocity wing in the [NII]λ6583 emission line observed in the SALT spectra sampling diffuse regions of VV 655. This feature is not seen in the Hα or [SII] lines, indicating that it is a faint feature originating in gas with a high N_2 ratio. It has a maximum offset of ~100 km s^{-1} from the peak emission, and it reaches to an average observed velocity of $v_{[NII]} = 2305 \pm 10$ km s^{-1} across the body of VV 655. Varenius et al. (2017) model the HI emission in this galaxy with a blue and a red component; the latter is centered at $v_{HI} = 2222.8$ km s^{-1} with a full width at half maximum of 29.8 km s^{-1}, and thus HI is not detected at the maximum [NII] velocity within the errors. While it is possible that HI with column densities below the detection threshold is associated with the redshifted wing, there is no evidence for an interaction between the ionized wing and the HI in the present data.

In the left panel of Fig. 4, we decompose the [NII]λ6583 emission line observed in r1 into two Gaussian components, one of which represents the redshifted wing. We find $N_2 \gtrsim 0.2$ for the high-velocity gas in both r1 and r3, and thus this component arises from gas with an N_2 intensity ratio at least a factor of two higher than is characteristic of VV 655, as often occurs when gas is shock heated (e.g., Payne et al. 2007, 2008; Newman et al. 2014). This combination of a redshifted velocity wing and possible shock excitation is consistent with ionized gas outflows from star-forming regions of dwarf galaxies. We note that these velocities may also arise from chemically enriched, infalling gas associated with a multi-phase galactic fountain flow or material stripped from VV 655 and/or NGC 4418 via their interaction.

Using the baryonic Tully-Fisher relationship and assuming an inclination of $\gtrsim$45° based on the isophotal axis ratio, we estimate a rotation speed $v_{\rm rot} \approx 90\,{\rm km\,s^{-1}}$ for VV 655 given the calibration of Bell & de Jong (2001). Thus, if the redshifted velocity wing is indicative of an outflow, the gas may require assistance from tides and ram pressure to escape the galaxy, potentially aiding the donation of mass and metals to NGC 4418 (see Bustard et al. 2018). Given the ongoing interaction and extended tidal debris associated with VV 655, gas escape aided by the interaction is a reasonable possibility (McClure-Griffiths et al. 2018), although gas confinement by ram pressure may also occur (Marcolini et al. 2003; Bustard et al. 2018).

4. A close passage of VV 655 by NGC 4418: Consideration of timescales

The HI maps of Varenius et al. (2017) present the case for VV 655 to have made a close passage by NGC 4418 ~100–400 Myr in the past. This timescale is broadly consistent with the projected separation of the two galaxies on the sky (300 kpc) and their relative radial velocities ($\Delta v \approx 100\,{\rm km\,s^{-1}}$). Varenius et al. (2017) prefer a prograde model where the orbital angular momentum vector for VV 655 is roughly aligned with the rotation vector for NGC 4418. However, since the dynamical properties of NGC 4418 were not known at the time, they do not exclude a retrograde interaction. Transient, arm-like stellar density features on one side of a disk galaxy can originate from such prograde, minor interactions. For example, Helmi et al. (2003) and Purcell et al. (2011) discuss how interactions with low-mass satellites can be responsible for arm-like ring features in the outer disk of the Milky Way.

Following the discussion by Helmi et al. (2003), the limited angular extent of the outer arm in NGC 4418 and its curvature suggest that this is a relatively young feature. A tidal arm is expected to wrap up and circularize over approximately a rotation time, or a few $\times 10^8$ years; it will then be disrupted by differential rotation over several more rotation periods, suggesting an age of <1 Gyr. The outer arm may have originated in several ways during an interaction, including disturbance of disk material, as in the references above, or as a remnant of material captured from VV 655 (e.g., Mihos & Hernquist 1994), though the regularity of the outer isophotes of VV 655 at multiple wavelengths disfavor this scenario (see Fig. 2). While the available data do not suffice to fully illuminate the specific details of the dynamical event, the age implied for the outer arm is consistent with its formation during the close passage of VV 655.

Ohyama et al. (2019) analyzed an SDSS optical spectrum of the central regions of NGC 4418 to identify the components of its stellar populations(s) (see also Shi & Gu 2005). These authors show that the stellar spectrum can be reproduced by combining a recent "starburst" stellar component with an age of ~10 Myr with an older "postburst" population with an age of ~300–400 Myr that may result from an earlier, interaction-induced starburst. Older populations are also present that produce about 40% of the V-band central zone light. Thus, the optically visible stellar populations are suggestive of an event where the central star formation rate increased several hundreds of Myr in the past and has since remained active into the present, consistent with the close passage of VV 655 both fueling the nucleus of the LIRG and forming the outer arm. We note that optical data do not probe the deeply hidden region around the nucleus where a significant fraction of the radiated power is likely to originate, and thus do not offer reliable insights into the properties of a centrally located active starburst in NGC 4418.

Our analysis of nebular emission-line intensities establishes that the ionized gas in VV 655 has substantially lower metallicity than that in NGC 4418. The extended ionized medium in NGC 4418 cannot have come recently from VV 655; any gas transferred to the LIRG must have been in the galaxy for a sufficient time to be chemically enriched. A gas residence time of a few 100 Myr in NGC 4418 would be sufficient to enrich the gas in α-elements and products of CNO nuclear burning (see, e.g., Matteucci & Recchi 2001). Thus, this time span suffices for any ISM transferred from VV 655 at the time of closest approach to be processed through multiple stellar generations and enriched in chemical elements, consistent with the relative gas-phase chemical abundances of VV 655 and NGC 4418 and the presence of dust in the apparent outflow cone (e.g., Evans et al. 2003; Sakamoto et al. 2013).

5. Discussion and conclusions

The combination of a LIRG classification, post-starburst optical spectrum, and unusual polar dust plumes indicate that NGC 4418 is in a transitory evolutionary phase. These properties are generally understood to result from an infusion of gas into the central regions of galaxies. The resulting high-density ISM can support active star formation and potentially fuel a central supermassive black hole. The gas mass involved in the central activity in NGC 4418 is $\geq 10^9\,M_\odot$ based on the masses of the young stars and molecular gas (Lisenfeld et al. 2000; Ohyama et al. 2019), which sets a limit on the nature of potential gas donors.

Interactions are the most likely triggers for gas infall events in present day galaxies, and major mergers are well established to generate dense central concentrations of molecular gas and associated luminous central starbursts. NGC 4418, however, does not display the prominent tidal tails, shells, or substantial asymmetries in its stellar body that are associated with major mergers. A minor merger, while capable of producing the observed behavior (e.g., Mihos & Hernquist 1994; Hernquist & Mihos 1995), is also unlikely. Such a merger would have required the presence of a second, low-mass but gas-rich companion galaxy in addition to VV 655 that has since merged with the LIRG. While possible, this scenario has a low probability of occurrence given the rarity of galaxies with two gas-rich satellites that could supply the necessary $\sim 10^9\,M_\odot$ of ISM (Liu et al. 2011; Tollerud et al. 2011).

A second possibility, considered by Mapelli et al. (2015), is for gas to be transferred from VV 655 to NGC 4418. Models by Mapelli et al. (2015) indicate that gas capture from an orbiting satellite galaxy can occur but will be inefficient. They estimate that about 10% of the satellite's gas can be transferred and potentially migrate to the center of the primary system. In NGC 4418, this model suggests an initial gas reservoir of $\approx 10^{10}\,M_\odot$ in VV 655. This exceeds the estimated HI mass

associated with VV 655 from Varenius et al. (2017) by an order of magnitude. The lack of irregular ionized gas kinematics along the minor axis of NGC 4418 and the need for any accreted material to lose angular momentum to migrate to the nuclear regions of the LIRG are also potential challenges to this model.

The third scenario to consider is that the perigalacticon passage of VV 655, likely on a prograde orbit, perturbed the pre-existing ISM in NGC 4418 and led to its central concentration. A variety of models show that a satellite with an SMC-like mass, such as VV 655, can produce tidal torques that result in a significant inward migration of the initial gas disk (Pettitt et al. 2016; Ramón-Fox & Aceves 2019). Indeed, the possibility of an interaction-induced inflow of molecular gas in the nucleus of NGC 4418 was raised by Kawara et al. (1990) and González-Alfonso et al. (2012). Studies of the HI content of early-type galaxies reveal that gas masses in the range of $10^9\,M_\odot$ are relatively common (e.g., Noordermeer et al. 2005; Morganti et al. 2006; Oosterloo et al. 2007), with considerable circumgalactic reservoirs of cool gas comparable to those found in late-type galaxies also often associated with such systems (Zahedy et al. 2019). It is thus entirely plausible for NGC 4418 to have contained a substantial ISM prior to its interaction with VV 655, consisting largely of HI supporting low levels of star formation.

This class of models appears most likely to apply in the case of NGC 4418 as it requires fewer special circumstances than either of the other two scenarios and has the added advantage that the gas in an early-type galaxy is expected to be at least moderately metal-rich and dusty (Griffith et al. 2019). This is in contrast to the possibility discussed by Varenius et al. (2017) in which the nucleus of NGC 4418 is fed by ongoing accretion from VV 655's tidal debris. While it is possible that a gas transfer event occurred during close passage and the donated material has since been chemically enriched in NGC 4418, the simplest model suggests that this is not the primary mechanism responsible for the unusual nuclear properties of the LIRG.

The innermost zones of NGC 4418, however, are deeply obscured in our optical observations. The ionized gas chemical abundances derived from optical data do not necessarily reflect conditions in the innermost nuclear region, unless gas is circulating between the nucleus and its surroundings. The presence of dusty plumes associated with a galactic outflow suggests that the ISM is unlikely to be quiescent and unmixed (see Ohyama et al. 2019); however, the degree to which mixing can occur is uncertain. Thus, it merits consideration whether the nucleus of NGC 4418 could be metal-poor due to recently accreted material from VV 655.

The rich molecular-line emission from the core of NGC 4418 is well observed and allows us to test for dense, metal-poor gas. Investigations of relative molecular abundances by Lahuis et al. (2007) and Costagliola et al. (2015) emphasize the diversity of the molecular content, including the prominence of nitrogen-bearing molecules such as HCN. Sakamoto et al. (2013) and Costagliola et al. (2015) also point to the similarity between emission in the nuclear region of NGC 4418 and that from the massive merger Arp 220. These data indicate that the dense nuclear region of NGC 4418 is not deficient in ^{14}N. This is a strong constraint since VV 655 is observed to have a low abundance of this secondary element.

We conclude that a recent close passage between VV 655 and NGC 4418 affected the evolutionary trajectories of both galaxies. The unusual nuclear properties of NGC 4418 most likely result from internal inward migration of its ISM due to tidal torquing by VV 655 that occurred ~300 Myr in the past. This event led to the central starburst as well as the likely ongoing substantial growth of the supermassive black hole in NGC 4418 (see Sakamoto et al. 2013; Roche et al. 2015, and references therein). For its part, VV 655 is actively starforming; as tabulated in the SDSS `emissionLinesPort` catalog, its Hα equivalent width of ≈80 Å is consistent with a starburst, likely induced by the interaction. VV 655 has clearly lost gas due to the interaction, yet retains low metallicity in its ISM. The presence of a metal-enhanced outflow, possibly stronger in the past, may partially account for the low metallicity in this system.

In this scenario, the presence of extremely Compton-thick molecular gas around the nucleus of NGC 4418 is occurring in the late phases of its interaction with VV 655, ~300 Myr after the peak of the associated starburst event in NGC 4418. This process stands in contrast to cases such as Arp 220, where extreme nuclear column densities are associated with high-intensity starbursts in an ongoing major merger. The NGC 4418–VV 655 interaction therefore serves as a signpost for the potential of minor interactions to produce profound effects, including an extremely Compton-thick nucleus, long after the peak of a collisionally induced disturbance from a low-mass companion. This case study thus illustrates that minor interactions can have considerable consequences for the more massive galaxy, motivating further statistical studies and simulations to determine the physical conditions under which the primary galaxy undergoes such significant evolutionary effects.

Given the increase in galaxy interaction rates with redshift, it is important to understand how various interaction scenarios shape the ISM. The relative frequency of interactions between giant galaxies and low-mass companions underscores the importance of characterizing such systems at low redshift, where a spatially resolved understanding of their stellar populations, morphologies, and gas kinematics and chemical abundances inform the physics driving the evolution of similar systems in the early universe.

Acknowledgements. Some of the observations reported in this paper were obtained with the Southern African Large Telescope (SALT) as part of program 2014-2-SCI-052, P.I.: J. S. Gallagher. The continued support from "Team SALT" is greatly appreciated. We thank the anonymous referees for useful comments, and Hsiao-Wen Chen for helpful discussions. Y. Ohyama and K. Sakamoto received support by the Ministry of Science and Technology (MOST) of Taiwan, MOST 107-2119-M-001-026- (Y. O.) and MOST 107-2119-M-001-022- (K. S.). This study would not have been possible without access to archival data from the SDSS and KiDS, and we thank these teams for their contributions to the astronomical research community. Funding for SDSS-III has been provided by the Alfred P. Sloan Foundation, the Participating Institutions, the National Science Foundation, and the U.S. Department of Energy Office of Science. The SDSS-III web site is `http://www.sdss3.org/`. SDSS-III is managed by the Astrophysical Research Consortium for the Participating Institutions of the SDSS-III Collaboration including the University of Arizona, the Brazilian Participation Group, Brookhaven National Laboratory, Carnegie Mellon University, University of Florida, the French Participation Group, the German Participation Group, Harvard University, the Instituto de Astrofisica de Canarias, the Michigan State/Notre Dame/JINA Participation Group, Johns Hopkins University, Lawrence Berkeley National Laboratory, Max Planck Institute for Astrophysics, Max Planck Institute for Extraterrestrial Physics, New Mexico State University, New York University, Ohio State University, Pennsylvania State University, University of Portsmouth, Princeton University, the Spanish Participation Group, University of Tokyo, University of Utah, Vanderbilt University, University of Virginia, University of Washington, and Yale University. Based on data products from observations made with ESO Telescopes at the La Silla Paranal Observatory under programme IDs 177.A-3016, 177.A-3017, 177.A-3018 and 179.A-2004, and on data products produced by Target/OmegaCEN, INAF-OACN, INAF-OAPD and the KiDS production team, on behalf of the KiDS consortium. OmegaCEN and the KiDS production team acknowledge support from: Deutsche Forschungsgemeinschaft, ERC, NOVA and NWO-M grants, Target, the University of Padova, and the University Federico II (Naples). Members of INAF-OAPD and INAF-OACN also acknowledge support from the

Department of Physics & Astronomy of the University of Padova, and of the Department of Physics of Univ. Federico II (Naples). This publication makes use of data products from the Wide-field Infrared Survey Explorer, which is a joint project of the University of California, Los Angeles, and the Jet Propulsion Laboratory/California Institute of Technology, funded by the National Aeronautics and Space Administration. This work is based in part on observations made with the *Spitzer* Space Telescope and the Galaxy Evolution Explorer, which are operated by the Jet Propulsion Laboratory, California Institute of Technology, under contract with the National Aeronautics and Space Administration. This work has made use of NASA's Astrophysics Data System and the NASA/IPAC Extragalactic Database (NED) and Infrared Science Archive which are operated by the Jet Propulsion Laboratory, California Institute of Technology, under contract with the National Aeronautics and Space Administration.

References

Aalto, S., Hüttemeister, S., & Polatidis, A. G. 2001, A&A, 372, L29
Aalto, S., Monje, R., & Martín, S. 2007, A&A, 475, 479
Armus, L., Heckman, T., & Miley, G. 1987, AJ, 94, 831
Asplund, M., Grevesse, N., Sauval, A. J., & Scott, P. 2009, ARA&A, 47, 481
Balcells, M., van Gorkom, J. H., Sancisi, R., & del Burgo, C. 2001, AJ, 122, 1758
Bell, E. F., & de Jong, R. S. 2001, ApJ, 550, 212
Bustard, C., Pardy, S. A., D'Onghia, E., Zweibel, E. G., & Gallagher, J. S., III 2018, ApJ, 863, 49
Costagliola, F., Sakamoto, K., Muller, S., et al. 2015, A&A, 582, A91
Crawford, S. M., Still, M., Schellart, P., et al. 2010, in Observatory Operations: Strategies, Processes, and Systems III, Proc. SPIE, 7737, 773725
Curti, M., Cresci, G., Mannucci, F., et al. 2017, MNRAS, 465, 1384
Duprie, K., & Schneider, S. E. 1996, AJ, 112, 937
Evans, A. S., Becklin, E. E., Scoville, N. Z., et al. 2003, AJ, 125, 2341
Ferreiro, D. L., & Pastoriza, M. G. 2004, A&A, 428, 837
Gallagher, J. S., III, & Hunter, D. A. 1987, AJ, 94, 43
Garn, T., & Best, P. N. 2010, MNRAS, 409, 421
González-Alfonso, E., Fischer, J., Graciá-Carpio, J., et al. 2012, A&A, 541, A4
Griffith, E., Martini, P., & Conroy, C. 2019, MNRAS, 484, 562
Helmi, A., Navarro, J. F., Meza, A., Steinmetz, M., & Eke, V. R. 2003, ApJ, 592, L25
Hernquist, L., & Mihos, J. C. 1995, ApJ, 448, 41
Hunter, D. A., & Gallagher, J. S., III 1985, ApJS, 58, 533
Imanishi, M., Nakanishi, K., Yamada, M., Tamura, Y., & Kohno, K. 2010, PASJ, 62, 201
Kaviraj, S., Ting, Y.-S., Bureau, M., et al. 2012, MNRAS, 423, 49
Kawara, K., Taniguchi, Y., Nakai, N., & Sofue, Y. 1990, ApJ, 365, L1
Kennicutt, R. C., & Evans, N. J. 2012, ARA&A, 50, 531
Knierman, K. A. 2010, in Galaxy Wars: Stellar Populations and Star Formation in Interacting Galaxies, eds. B. Smith, J. Higdon, S. Higdon, & N. Bastian (San Francisco, CA: ASP), ASP Conf. Ser., 423, 342
Koda, J., Okuda, T., Nakanishi, K., et al. 2005, A&A, 431, 887
Koribalski, B., & Manthey, E. 2005, MNRAS, 358, 202
Kuijken, K., Heymans, C., Dvornik, A., et al. 2019, A&A, 625, A2
Lahuis, F., Spoon, H. W. W., Tielens, A. G. G. M., et al. 2007, ApJ, 659, 296
Lisenfeld, U., Isaak, K. G., & Hills, R. 2000, MNRAS, 312, 433
Liu, L., Gerke, B. F., Wechsler, R. H., Behroozi, P. S., & Busha, M. T. 2011, ApJ, 733, 62
Loose, H. H., & Thuan, T. X. 1986, in Star-forming Dwarf Galaxies and Related Objects, eds. D. Kunth, T. X. Thuan, J. Tran Thanh Van, J. Lequeux, & J. Audouze (Editions Frontières), 73
Lucero, D. M., & Young, L. M. 2013, AJ, 145, 56
Mapelli, M., Rampazzo, R., & Marino, A. 2015, A&A, 575, A16
Marcolini, A., Brighenti, F., & D'Ercole, A. 2003, MNRAS, 345, 1329
Matteucci, F., & Recchi, S. 2001, ApJ, 558, 351
McClure-Griffiths, N. M., Dénes, H., Dickey, J. M., et al. 2018, Nat. Astron., 2, 901
Mihos, J. C., & Hernquist, L. 1994, ApJ, 425, L13
Morganti, R., de Zeeuw, P. T., Oosterloo, T. A., et al. 2006, MNRAS, 371, 157
Newman, S. F., Buschkamp, P., Genzel, R., et al. 2014, ApJ, 781, 21
Nilson, P. 1973, Uppsala General Catalogue of Galaxies (Uppsala: Astronomiska Observatorium)
Noordermeer, E., van der Hulst, J. M., Sancisi, R., Swaters, R. A., & van Albada, T. S. 2005, A&A, 442, 137
Nyland, K., Young, L. M., Wrobel, J. M., et al. 2017, MNRAS, 464, 1029
Ohyama, Y., Sakamoto, K., Aalto, S., & Gallagher, J. S., III 2019, ApJ, 871, 191
Oosterloo, T. A., Morganti, R., Sadler, E. M., van der Hulst, T., & Serra, P. 2007, A&A, 465, 787
O'Sullivan, E., Combes, F., Salomé, P., et al. 2018, A&A, 618, A126
Payne, J. L., White, G. L., Filipović, M. D., & Pannuti, T. G. 2007, MNRAS, 376, 1793
Payne, J. L., White, G. L., & Filipović, M. D. 2008, MNRAS, 383, 1175
Pearson, S., Privon, G. C., Besla, G., et al. 2018, MNRAS, 480, 3069
Pereira-Santaella, M., Rigopoulou, D., Magdis, G. E., et al. 2019, MNRAS, 486, 5621
Pettitt, A. R., Tasker, E. J., & Wadsley, J. W. 2016, MNRAS, 458, 3990
Pisano, D. J., & Wilcots, E. M. 1999, AJ, 117, 2168
Purcell, C. W., Bullock, J. S., Tollerud, E. J., Rocha, M., & Chakrabarti, S. 2011, Nature, 477, 301
Ramón-Fox, F. G., & Aceves, H. 2019, MNRAS, 491, 3908
Roche, P. F., Aitken, D. K., Smith, C. H., & James, S. D. 1986, MNRAS, 218, 19P
Roche, P. F., Alonso-Herrero, A., & Gonzalez-Martin, O. 2015, MNRAS, 449, 2598
Sakamoto, K., Aalto, S., Evans, A. S., Wiedner, M. C., & Wilner, D. J. 2010, ApJ, 725, L228
Sakamoto, K., Aalto, S., Costagliola, F., et al. 2013, ApJ, 764, 42
Sancisi, R., Fraternali, F., Oosterloo, T., & van der Hulst, T. 2008, A&ARv, 15, 189
Shi, L., & Gu, Q.-S. 2005, Chin. J. Astron. Astrophys., 5, 117
Spoon, H. W. W., Keane, J. V., Tielens, A. G. G. M., Lutz, D., & Moorwood, A. F. M. 2001, A&A, 365, L353
Tollerud, E. J., Boylan-Kolchin, M., Barton, E. J., Bullock, J. S., & Trinh, C. Q. 2011, ApJ, 738, 102
van Dokkum, P. G. 2001, PASP, 113, 1420
van Zee, L. 2001, AJ, 121, 2003
Varenius, E., Costagliola, F., Klöckner, H.-R., et al. 2017, A&A, 607, A43
Zahedy, F. S., Chen, H.-W., Johnson, S. D., et al. 2019, MNRAS, 484, 2257